Optimizing the Global Digital Elevation Models (GDEMs) and accuracy of derived DEMs from GPS points for Iraq's mountainous areas

Shazad Jamal Jalal [a, b, *], Tajul Ariffin Musa [a], Taher Hama Ameen [c], Ami Hassan Md Din [a], Wan Anom Wan Aris [a], Jwan Mohammad Ebrahim [d]

[a] Faculty of Built Environment and Surveying, Universiti Teknologi Malaysia, Johor Bahru, 81310, Malaysia
[b] College of Engineering, University of Sulaimani, 46001, Sulaimani, Iraq
[c] University of Arkansas at Little Rock, Little Rock, 72204, AR, USA
[d] SALP Middle East Ltd. Company for Oil and Gas Pipeline Construction, Erbil, Iraq

ARTICLE INFO

ABSTRACT

Optimizing the combined horizontal and vertical accuracy of the well-known Global Digital Elevation Models (GDEMs) of various resolutions for each country and region especially in Iraq's mountainous areas is still questionable. All the three GDEMs, approximately, have the same vertical accuracy with the Root Mean Square (RMSE) of ± 7.3 m, ± 7.6 m and ± 6.5 m via 12 fixed Ground Control Points (GCPs) for the Advanced Land Observation Satellite Phased Array L-band Synthetic Aperture Radar (ALOS PALSAR 12.5 m), the Shuttle Radar Topographic Mission (SRTM 30 m) and the TerraSAR-X (the name of twin satellites) add-on for Digital Elevation Measurement (TanDEM-X 90 m) GDEMs respectively. Moreover, the percentage of outliers that are greater or smaller than ± 10 m detection of the height extraction from both the ALOS PALSAR and SRTM Digital Elevation Models (DEMs) contains 16.7% and for TanDEM-X was 25%. In this paper, the special DEM is derived using 2123 handheld GPS points for Sulaymaniyah Governorate, Kurdistan region, Iraq. The height extraction by discarding the outliers of 58% gives the RMSE of ± 8.0 m in the case of adding geoid heights (N) to the ellipsoidal heights (h) via the Earth Gravitational Model 2008 (EGM2008) and ± 5.6 m without adding N. It is expected that the derived DEMs will give more accurate results both horizontally and vertically in the mountainous areas when GPS observations are intensified. The horizontal accuracy is validated through extracting hierarchy stream types of the watershed map from the DEMs for higher than 100 pixels length. The ALOS PALSAR DEM extracted more numbers of stream orders than others. Finally, based on the criteria of RMSE, outlier detection, and the number of extracted stream orders, the ALOS PALSER DEM is regarded as the optimal GDEM in comparison with the close accuracy of both the TanDEM-X and SRTM DEM.

1. Introduction

There are three common methods for computer representation of terrain of the Earth, namely, the Digital Elevation Model (DEM), the Triangulated Irregular Network (TIN), and the contour-based model. In the DEM method, the terrain is divided into regular cells, whilst in the TIN method the terrain is covered and connected with irregular triangles. The contour-based model produces irregular patch shaped surfaces using the intersection of a set of lines normal to the contour and the lines with the steepest descents [1].

The DEM is a quantitative representation of the Earth's surface and spatial information of data which has become a vital source of information about the elevation, slope and terrain relief for scientific investigations and researchers. It replaces the traditional paper-based topographical data sources and formats. It also takes up data structures for storing, displaying and analyzing the topographical information. The interpolation is used to establish the

* Corresponding author. Faculty of Built Environment and Surveying, Universiti Teknologi Malaysia (UTM), Johor Bahru, 81310, Malaysia.
E-mail addresses: shazad.jalal@univsul.edu.iq, shazadjj@gmail.com (S.J. Jalal).

elevation value for the entire terrain. The elevation value is related to an array representation of square cells or pixels. The DEM can be derived from a variety of sources such as the interpolation of contour lines, existing topographic maps, field surveys and photogrammetry, with the field survey being the most accurate in comparison to the other sources. The DEM can also utilize data from new methods such as the aerial stereo-photogrammetry, satellite remote sensing, radar interferometry, airborne laser scanning and radar altimetry [2–7].

The extracted land−surface parameters from the DEMs vary with a spatial scale which is a function of cell size or grid resolution. Normally, the higher the DEM resolution the more accurate results. Therefore, the determination optimal cell resolution of the DEMs has been a topic of research in the last of the previous decade [8,9].

The Shuttle Radar Topographic Mission (SRTM) of $1'' \times 1''$ resolution (approximately 30×30 m), is the most popular GDEM freely available from the National Aeronautics and Space Administration (NASA) and covers latitudes between 56°S and 60°N. However, it is unsuitable for mapping metropolitan areas [7,10–13]. On the other hand, the TerraSAR-X (the name of twin satellites) add-on for Digital Elevation Measurement (TanDEM-X 90 m) product of an arc $3'' \times 3''$ resolution (approximately 90×90 m) is freely downloadable online for scientific use which is available as a database now and represents the bare Earth surface. However, the Advanced Land Observation Satellite Phased Array L-band Synthetic Aperture Radar (ALOS PALSAR 12.5 m) is the most precise GDEM in the world and opened for free to the public since 2015 [14].

The DEM inherent different types of errors such as gross errors in data collection and deficient orientation of stereo images with unknown combination errors and unknown sources. These errors vary depending on the geographical locations, grid spacing, and the interpolation techniques used to derive the DEM. With all these types of errors, the main limitations of the DEM are under-sampling rough areas and oversampling flat areas [1,6].

A quality of the DEM is influenced by several factors, including algorithm, terrain type, grid spacing and characteristics as well as sensor types [15]. The validation of such GDEMs in different countries and regions would give more benefits to global users due to the various accuracy of these DEMs over the different regions [16]. The first step of assessing the quality of the DEM is to check a sample of suitable numbers of heights from the DEM against known heights. The problem of assessing the DEM based on a limited sample of check points is because of impossible determination, whether the type of error is systematic/random or blunders. Therefore, hydrological analyses including derivation of watersheds will be another indication which is largely sensitive to the DEM quality [17].

Researches have shown that the Global Navigation Satellite Systems (GNSS), including the Global Positioning System (GPS), is capable of providing the accurate and continuous three-dimensional positioning to users at all local, regional, national and international scales [18]. Therefore, the GPS observations could potentially replace the classical surveying instruments [19].

Although the GPS allows for the fast and accurate location information (e.g. latitude, longitude and elevation) of points depending on the World Geodetic System 1984 (WGS84), it measures the ellipsoidal height (h) instead of the orthometric height (H) which is needed in various engineering applications and mapping. The H values can be measured using spirit leveling, or by the terrestrial leveling process which is time-consuming and costly especially in rough and mountainous areas [20].

The GPS leveling needs a height correction to be algebraically added to the value of h to obtain the value of H. This correction is known as the geoid height or geoidal undulation (N). The values of N are typically in the range of ±100 m. A positive value of N indicates that the geoid is above the ellipsoid, whilst a negative value indicates the opposite. The maximum measured value of N is +80 m close to New Guinea, in the Andes Mountains and the southwest of the Indian Ocean. Whereas, the minimum value of N is −105 m measured in different locations including near Puerto Rico, Sri Lanka, the west of California and Antarctica [21].

The main objective of the study is to determine the relationship between the resolution of the global well-known DEMs and their vertical accuracy for Iraq's mountainous areas. Accordingly, the best DEM will be identified for different application usages. Another objective is to examine the accuracy of the extracted DEM from handheld GPS points in comparison to the same global DEMs of the study area. This effort is considered as the first study of its kind for optimizing the three GDEMs in Iraq and its mountainous areas.

2. The study area

The study area is Sulaymaniyah Governorate, which is a part of a mountainous area in the Kurdistan region of Iraq. The area is located in the Universal Transverse Mercator (UTM) zone 38° N and surrounded by latitudes 34.7°N-36.5°N and longitudes 44.5°E-46.3°E (Fig. 1). The whole area is estimated to be 17,023 km², which accounts for 3.9% of the total area of Iraq [22,23].

The area is characterized by its mountainous and rolling areas, and comprises four mountain series, wide areas of fertile plains and no desert. A part of Zagros Mountain representing the highest mountain series is located at the north-east of the study area which forms a natural border with Iran and extends toward Iran itself. Another part of the Zagros Mountain series extends from the north towards the north-east. The third series is Peramagroon Mountains, which is located few kilometers north of Sulaimani city (the capital or the center of Sulaymaniyah Governorate) and it trends southeast towards the north-west. Finally, the Baranan Mountain series, which is relatively lower than the others, extends from the south-west towards the north-east [24].

The study area has many limitations that restrict terrestrial land surveying. It contains a wide risky area of land mines and unexploded bombs from the Iraq−Iran war, especially along with the mountainous belts of the border with Iran. The most recorded numbers of mine victims in Iraq are in Sulaymaniyah Governorate of about 8130 victims until 2017 [25]. Furthermore, the north-east and south-east borders of Sulaymaniyah Governorate is on top of the mountainous area that forms the common border with Iran and is prohibited from civilians to get in. Generally, there is a difficulty to reach the top of mountains due to the unsuitability of existing earth roads.

These severe constraints have made the terrestrial land surveying carried out in the current study to be limited to measuring points around the mountains. Attempts were made to collect data on top of the mountains using a helicopter, however, only a limited amount of information could be collected due to the associated cost of taking a helicopter flight, and restrictions on helicopter departure in the rugged mountains of the remote areas.

3. Methodology

Different datasets and methods were used for both extracting the GDEMs and deriving the DEMs from the GPS points for the study area. These are explained in the following sections.

3.1. GDEMs extraction

The extraction method of each GDEM as well as DEM from the GPS points for the study area can be summarized as follows (Fig. 2).
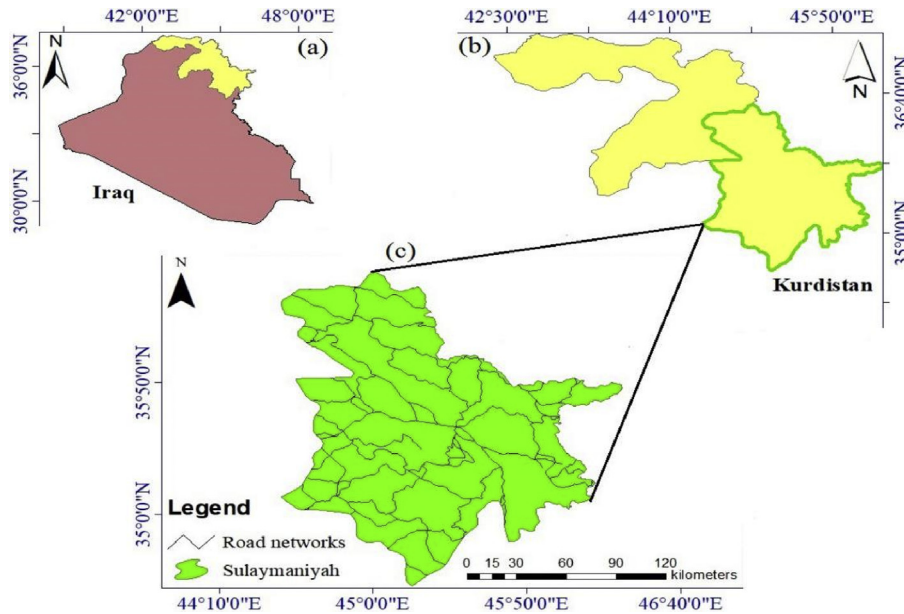
Fig. 1. The geographical locations of (a) Kurdistan region in Iraq, (b) the study area in Kurdistan region and (c) the study area (source: prepared and drawn by the researchers).

1) Extracting ALOS PALSAR DEM:
   A) Select the study area to download the Advanced Land Observation Satellite Phased Array band Synthetic Aperture Radar (ALOS PALSAR) with long frequency and a spatial resolution of 12.5 × 12.5 m from the Vertex website (http://vertex.daac.asf.alaska.edu/).
   B) Choose Dual Beam Fine (DBF) sensor. Then, select the high-resolution option to download the DEM.
   C) Export the downloaded DEM to the ArcGIS10.5.

2) Extracting SRTM DEM:
   A) Select the study area to download the SRTM with medium frequency and a spatial resolution of an arc 1″ × 1″ (approximately 30 × 30 m) from the Earthexplorer website (https://earthexplorer.usgs.gov/).
   B) Export the downloaded DEM to the ArcGIS10.5.

3) Extracting TanDEM-X:
   A) Select the study area to download the TanDEM-X with short frequency and a spatial resolution of 3″ × 3″ (approximately 90 × 90 m) from the Earth Observation Center (EOC) of the German Aerospace Center (DLR) website (https://geoservice.dlr.de/web/maps).
   B) Export the downloaded DEM into the ArcGIS10.5.

4) Extracting GPS points DEM:
   A) Export the coordinates of points and their elevations from the Excel sheet to the ArcGIS10.5.
   B) Choose the Inverse Distance Weighted (IDW) for the interpolation because this method gives the best result for generating the DEM and it is more accurate than the Kriging method of the interpolation [26].

Finally, each above product is clipped as a study area separately. Then, the sink and fill commands are applied for each to extract the four above DEMs respectively.

3.2. GPS observations

A handheld GPS (Garmin GPSMAP 60CSx) was used for the current fieldwork. This type of GPS is preferred to the commonly used
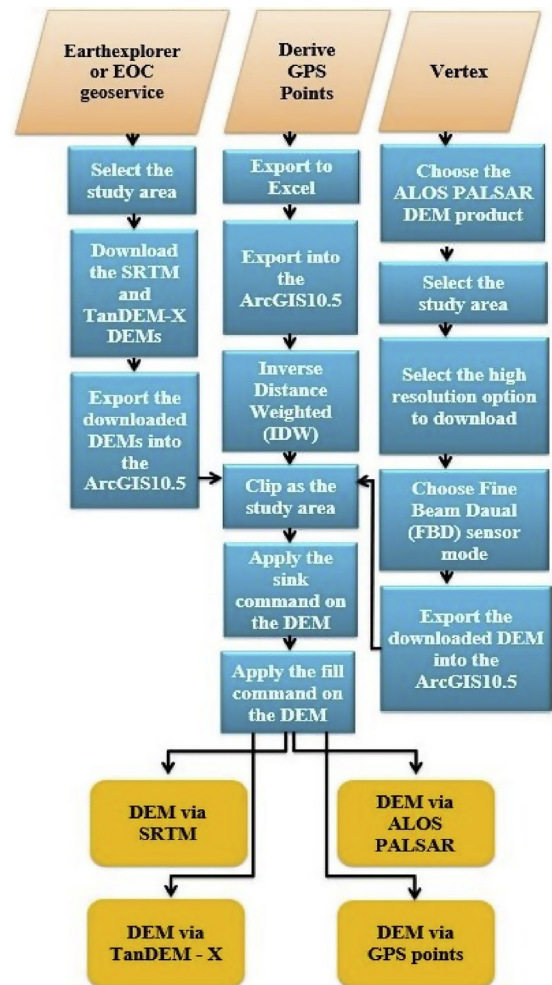

Fig. 2. Flowchart of extracting SRTM and ALOS PALSAR DEMs,TanDEM-X and derived DEMs from the handheld GPS points for the study area.

Garmin handheld GPS due to its higher sensitivity and accuracy for these types of works. Measurement accuracy using the Differential GPS (DGPS) with code data is < 5 m and <10 m for horizontal and vertical measurements, respectively [27]. However, the Ground Control Points (GCPs) (also called GPS leveling points) observed accurately using the static GPS survey and geodetic receivers to be in use for validating the DEMs as discussed in section 3.5.

Two datasets are used in the current study for deriving the DEM using the GPS points. The main dataset is obtained from the comprehensive fieldwork of GPS observations carried out in this study which covers the entire study area. This dataset was supplemented by a secondary set of data which was taken from the works of previous researchers carried out between 2007 and 2010, and contains the density of points for a limited area. The overall number of points within the study area is 2123 as shown in Table 1 and Fig. 3 [28−31].

Table 1
Specification of the handheld GPS observations datasets.

No.	Source of dataset	Characteristics of the GPS points	Information	Total points
1	Fieldwork (Researchers)	Year of survey	2018	166[1]
		Distance between the points	<11 km	
2	Ph.D. Thesis [28]	Year of survey	2010	1315
		Distance between the points	0.5−1 km	
3	M.Sc. Thesis 1 [29]	Year of survey	2008	206
		Distance between the points	0.5−1 km	
4	M.Sc. Thesis 2 [30]	Year of survey	2008	319
		Distance between the points	0.5−1 km	
5	Unpublished data [31]	Year of survey	2008	**117**
		Distance between the points	5−10 km	
	Total GPS points			2123

Note:
[1] 161 out of 166 points were surveyed using the Sport Utility Vehicle (SUV) and the rest 5 points were surveyed by the helicopter.

3.3. Fieldwork

Before starting the fieldwork of the GPS survey as shown in Fig. 4, a reconnaissance survey is conducted covering the basic information about the whole study area and its main and accessible routes. Traveling routes were carefully selected to avoid repetition and save cost and time for the GPS observations. However, the SUV with a four wheel drive (4WD) struggled to reach the top of the mountains, hence, the helicopter was utilized to measure a limited number of points on a selected top of a mountain series (see Fig. 3).

The total number of the GPS points was 166 in which 5 points were measured using the helicopter as presented in Table 1 and Fig. 3. The average distance between points was 11.8 km with 56% of the distance intervals being greater than 10 km as given in Table 2. Whereas, the average distance between the GPS points of previous works ranges between 0.5 km and 1 km as shown in Table 1.

The comprehensive GPS fieldwork covered the entire study area. The overall distance of the field survey was 5526 km back and forth via the SUV and 120 km via the helicopter over a part of the Baranan Mountain series (as described in section 3.1). Triangulation networks were constructed for all the 166 GPS points using the Autodesk Inc.'s AutoCAD Civil 3D 2019 software. The number of triangles in the triangulation networks between the connected gravity points was 305 and the number of lines without repetitions was 470 as shown in Fig. 5.

3.4. Extracting the geoid heights from the Earth Gravitational Model

The Earth Gravitational Model 2008 (EGM2008) was used for extracting the N values for the GPS points to convert them to H which is released by the EGM development team from the U.S. National Geospatial-Intelligence Agency (NGA), and it is publicly available from their website. This model is complete to the
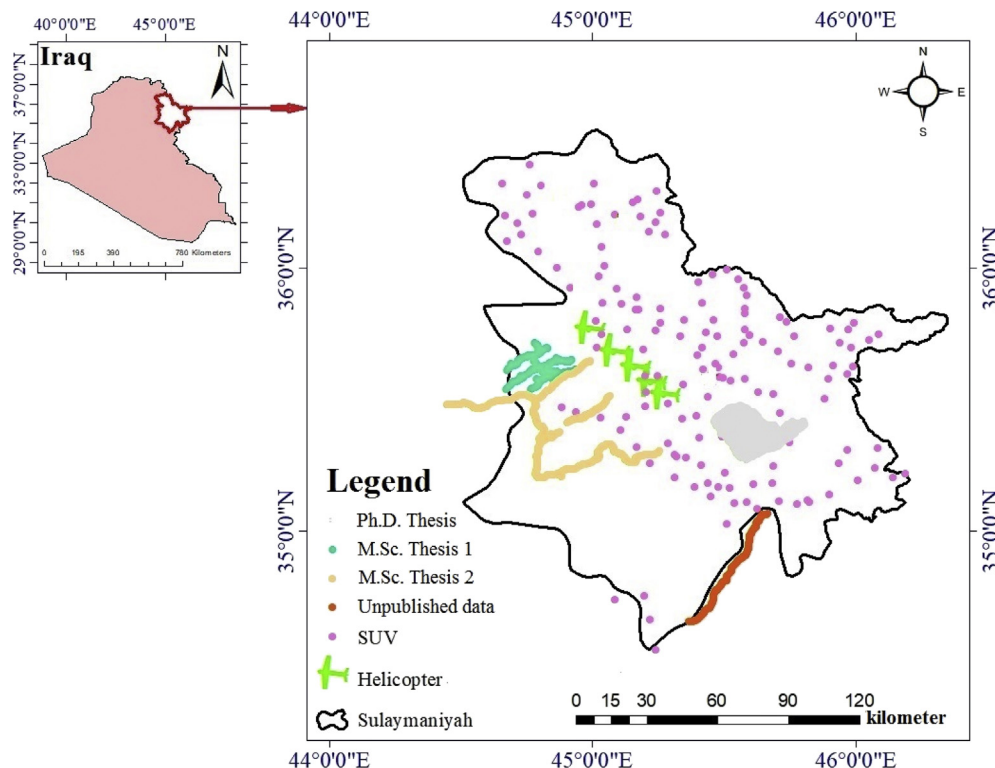

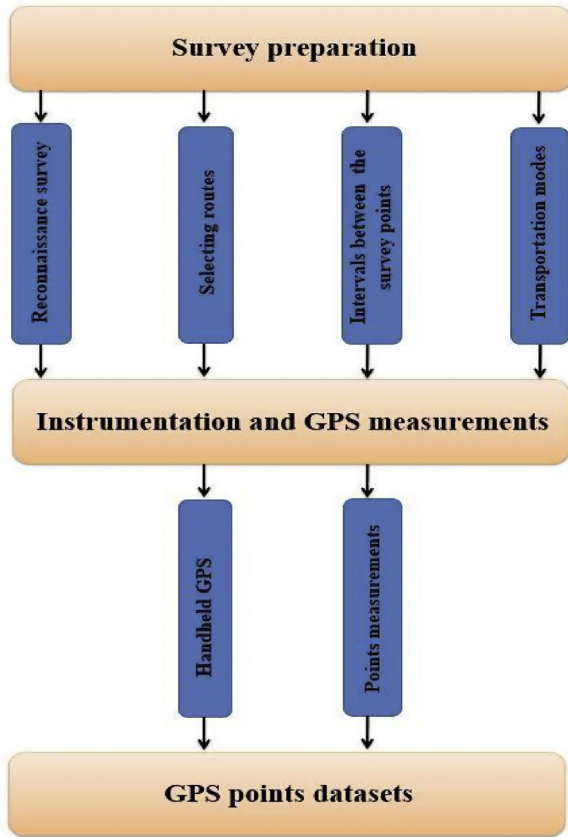**Fig. 3.** Datasets of the GPS points in the study area.

Fig. 4. Flowchart of conducting the handheld GPS survey.

Fig. 5. The triangulation networks between the surveyed handheld GPS points inside the study area.

heights obtained from the DEMs via Root Mean Square Error (RMSE) as shown in Eq. (1) [17]. The validation technique via GCPs was conducted earlier by the United States and Japanese partners for the validation and characterization of the Advanced Space-borne Thermal Emission and Reflection Radiometer Global Digital Elevation Model (ASTER GDEM) [33].

$$RMSE = \sqrt{\frac{\sum_{i=1}^{n}[X(\text{predicted}) - X(\text{measured})]^2}{n-1}} \qquad (1)$$

where,

RMSE: value of root mean square error,

X(measured): elevation of the GCPs,

X(predicted): extracted heights of the same positions of GCPs from the GDEMs,

n: number of the GCPs.

These national GCPs include two sets which were established by the Polish Polservice Company between 1974 and 1977 [34]. They were later accurately observed and processed by the Iraq General Board of Surveying (GBS) using the static GPS survey and geodetic receivers in 2008. The Online Positioning User Service (OPUS) report files for the national GCPs were provided by the National Geodetic System (NGS) website. The accuracy of horizontal control ranged between 1 cm and 4 cm. However, the accuracy of h ranged between 1 cm and 11 cm as shown in Table 3.

The first set of the GCPs contains 10 previous benchmarks (BMs) which were the first-order benchmarks of ±0.1 mm accuracy. Whereas, the other set consists of 5 previous triangulation points and their H were measured using the trigonometric leveling based on the nearest first-order benchmarks around them. However, the accuracy of these triangulation points is from ±30 cm−50 cm because of the refraction errors of a theodolite during the observations (see Table 3) [34].

spherical harmonic degree and order 2159 and contains an additional coefficients extending to degree 2190 and order 2159 [32].

For countries such as Iraq, which lacks its local geoid, the EGM2008 can be used as a source to formulate the global geoid model for computing the geoid heights (N) according to the WGS84 for the entire Earth. Therefore, each observed ellipsoidal height (h) via the Garmin handheld GPS was converted to H through the extracted N from the EGM2008. The converted orthometric heights were then used for deriving the DEMs from the GPS points of the study area as illustrated in Fig. 2.

3.5. GCPs

The GCPs are crucial for validating and selecting the best DEMs based on their actual measured orthometric heights and predicted

Table 2
Average distance interval between the handheld GPS points in the study area.

No.	Distance interval (km)	No. of lines	Percentage of distance intervals (%)
1	<5	56	12
2	5 to < 10	208	44
3	10 to < 15	115	25
4	15 to < 20	44	9
5	>20	47	10
	Total	470	100

Note: (1) The average distance interval among the GPS points is 11.8 km.
(2) The total number of possible triangle networks among the GPS points is 305.
(3) The total number of sides among the GPS points without repetitions is 470.
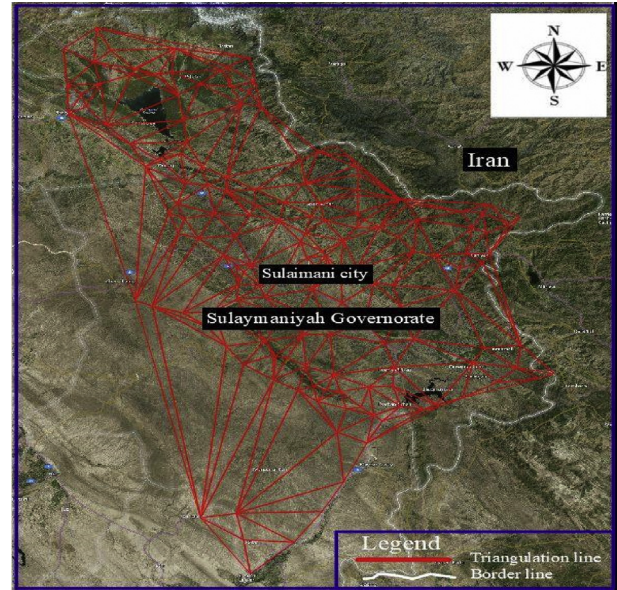
Table 3
The h and H values with their accuracies of the GCPs.

No.	GCP Code	h (m)	H (m)	σ_h (cm)	σ_H (mm or cm)
1	35−10	880.32	872.45	3	0.01 mm
2	35−12	714.84	707.16	11	0.01 mm
3	35−17	875.90	867.16	6	0.01 mm
4	36−30	520.30	513.48	4	0.01 mm
5	36−34	702.84	695.96	5	0.01 mm
6	36−43	693.20	684.65	2	0.01 mm
7	43−11	522.10	512.95	1	0.01 mm
8	43−12	650.81	640.11	7	0.01 mm
9	43−17	661.86	650.26	1	0.01 mm
10	H4[a]	526.63	516.17	−	0.01 mm
11	9019	−	864.6	−	0.3−0.5 cm
12	10002	−	1712.3	−	0.3−0.5 cm
13	10016	−	1232.7	−	0.3−0.5 cm
14	10037	−	614.9	−	0.3−0.5 cm
15	10039	−	1118.6	−	0.3−0.5 cm

Note: h means ellipsoidal height, H means orthometric height, σ means standard error, σ_h means the standard error of the ellipsoidal height and σ_H means the standard error of the orthometric height of the GCPs.

[a] The H of GCP H4 is measured by the researchers directly using sprit leveling, based on the benchmark which is located on the body of Dukan dam.

3.6. Watershed mapping

Hydrological or watershed mapping is another method for validating the horizontal accuracy of both the GDEMs and derived DEMs from the GPS points. In the current study, each DEM via ArcGIS10.5 was utilized for deriving watershed maps for the study area which is represented by the main streams of accumulation thresholds of greater than 100 pixels (as proposed by Wise [17]) according to each extracted DEM as shown in Fig. 6.
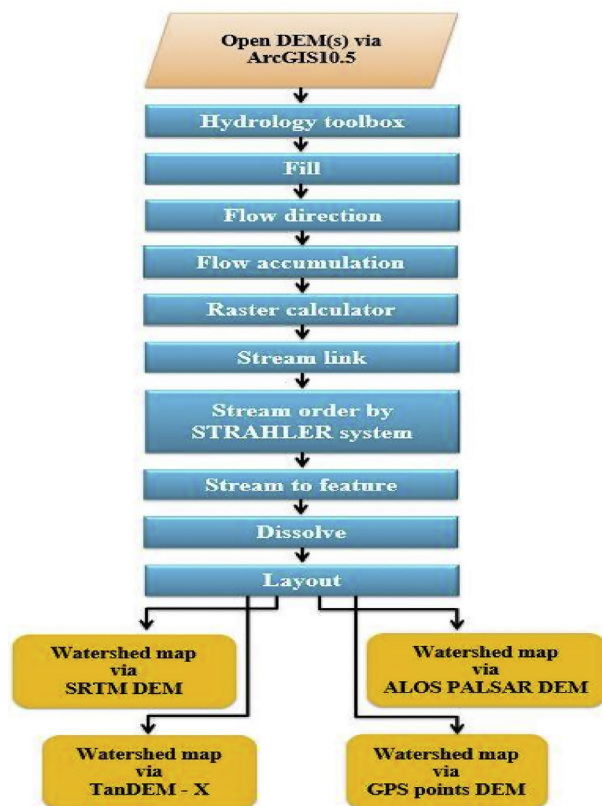

Fig. 6. Flowchart of extracting watershed mapping from the SRTM and ALOS PALSAR DEMs, TanDEM-X as well as the derived DEMs from the handheld GPS points.

Therefore, higher numbers of the stream orders with more resolution in the watershed map via the exact DEM will be the optimal GDEM for the study area. Accordingly, the resolution of the derived DEMs from the GPS points will be also assessed for the study area.

4. Results and discussions

The GDEMs with different resolutions include the SRTM and ALOS PALSAR DEMs, TanDEM-X as well as the derived DEMs from the GPS points for the study area as shown in Fig. 7. The horizontal reference of all the GDEMs is all the same and referenced to the WGS84. However, the vertical reference of the ALOS PALSAR and SRTM DEMs are both referenced to the Earth Gravitational Model 1996 (EGM96) and the obtained height from both the DEMs is H as shown in Table 4. On the other hand, the extracted height from the TanDEM-X is different and represents the h in which it needs to synchronize to be the H by algebraic adding of N via Eq. (2) [13].

$$N_{Geom} = h - H \tag{2}$$

Where,

N_{Geom} means geometric geoidal height, h means ellipsoidal height and H means orthometric height.

The results show that the minimum and maximum elevations of the terrain via DEMs vary from 238 m to 3019 m in the SRTM DEM, 244 m to 3041 m in the ALOS PALSAR DEM, and 246 m to 3039 m in the TanDEM-X. The differences in elevation (ΔH) between the maximum and minimum heights are 2781 m, 2797 m and 2793 m in each of the ALOS PALSAR and SRTM DEMs as well as the TanDEM-X respectively. However, the minimum and maximum elevations of the derived DEMs from the GPS points range between 279 m and 1679 m with a ΔH of 1400 m (see Table 4). Recently, a related study which carried out in the plain area of Iraq at the University of Baghdad Campus [35], and identified the roughness of the Earth surface and density of collected data are the main factors controlling the quality of the derived DEMs via the handheld GPS points. Hence, the study used density points in a limited and flat area (0.8 × 1.0 km) to achieve a better accuracy for the derived DEMs via the handheld GPS points. Therefore, this discrepancy between the GDEMs and the derived DEMs is because of the limited number of GPS points used in the current study and excluding the mountainous series with the highest points especially the Iraq−Iran border mountains. The plain areas were not covered in the south-west of the study area in which the lowest points are located.

4.1. Validating GDEMs via GCPs

It is necessary to evaluate the accuracy of the DEMs obtained before they can be used in the future. Results of research carried out on the northern margin of the Tibetan Plateau have demonstrated that the standard error of the GCPs of ASTER GDEM of a spatial resolution of 1″ × 1″ is 9.3 m with a precision of 10 m for the whole area [35]. Previous researches also identifies outliers as values outside the range of ±10 m (more or less than 10 m) for the accuracy of half of the contour interval for mountainous areas with maps of scale 1/20,000 and contour intervals of 20 m [36,37]. This range margin of ±10 m is utilized as a guide to assess the accuracy of the obtained DEMs and to highlight the detected outliers.
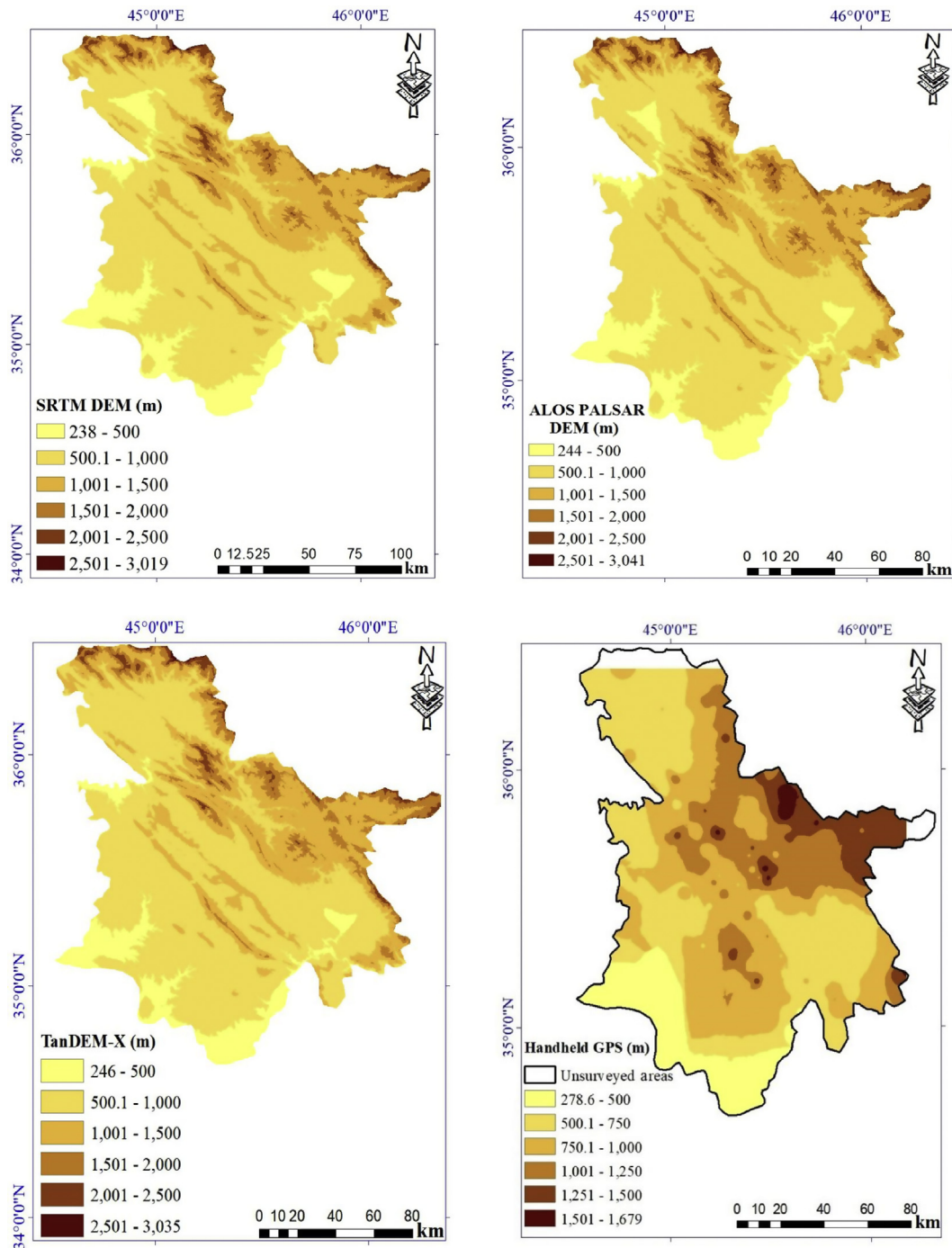
Fig. 7. Extracting the SRTM and ALOS PALSAR DEMs, TanDEM-X as well as the derived DEMs from the handheld GPS points for the study area.

Table 4
Specifications and elevation ranges of the GDEMs in the study area.

No.	Name of the GDEM	Reference system [13,14]		Spatial resolution (m)	Minimum and maximum elevation (m)	Range (m)
		Horizontal	Vertical			
1	ALOS PALSAR	WGS84	EGM96	12.5	244 and 3041	2797
2	SRTM	WGS84	EGM96	30	238 and 3019	2781
3	TanDEM-X	WGS84	WGS84	90	246 and 3039	2793

Based on Table 5, the RMSEs of the height discrepancies of the ALOS PALSAR and SRTM DEMs as well as the TanDEM-X with the heights of GCPs show ±7.3 m, ±7.6 m and ±6.5 m, respectively, with a slight insignificant difference between them. The correlation coefficient (r) is used to quantify correlations between variables measured in this study. The value of r ranges between +1 (for perfect, direct correlation) and −1 (for perfect, inverse correlation), with a value of zero showing no correlation between the variables [38]. In Table 6, the value of r for the RMSE, has a strong relationship with height values of +0.73 m and +0.70 m for both the ALOS PALSAR and SRTM DEMs. Fig. 8 which is utilized via MATLAB shows that the number of detected outliers (10 m or more) based on the height of 12 GCPs was 1 (8%) in the TanDEM-X and 2 (16%) in both the ALOS PALSAR the SRTM DEMs. According to the detected outliers, the TanDEM-X is the best GDEM because it has the minimum number of outlier.

4.2. Validation of the derived DEMs from the GPS points via GCPs

The GPS observations and post-processing of the GCPs were carried out by the Iraqi General Board of Surveying. The difference between the geometric geoid heights (N_{Geom}) of GCPs is the algebraic difference of the h and the H (see Eq. (2)). Based on Table 7, the value of N_{Geom} of GCPs in the study area is positive and varies between +6.82 m and +11.60 m.

Two DEMs for the GPS points have been derived via EGM2008 for obtaining N values of the points. A DEM was derived through adding N correction to h and another DEM was derived without adding N values. When outliers are excluded, the obtained RMSE of discrepancies with no N correction to the DEM is better than the DEM with N corrected, because of the accuracy of the handheld GPS itself (less than 10 m is also within the limit of outlier range) which is equivalence to the N values (from +6.82 m to +11.60 m) within the study area (see Table 7). In other words, if the N value corrections are added, the amount of error in H values will increase due to the accuracy of the handheld GPS used in this study.

RMSE of discrepancies for the GDEMs is larger than the derived DEMs from GPS points without adding N values except for the SRTM DEM. In the ALOS PALSAR and SRTM DEMs as well as the TanDEM-X, the RMSE of discrepancies are 8.5 m, 3.6 m and 9.2 m,

Table 6
Minimum and maximum elevation discrepancies of the GCPs via the GDEMs in the study area.

Statistical indicators	ALOS PALSAR (m)	SRTM (m)	TanDEM-X (m)
Minimum discrepancy	1	1	0
Maximum discrepancy	11	18	13
Correlation coefficient (r) between H and the discrepancy	0.73	0.70	0.46

respectively, whereas 5.6 m and 8.2 m were recorded in both the derived DEMs from the GPS points as shown in Table 8.

4.3. Validating the GDEMs and derived DEMs from GPS points via watershed maps

Four watershed maps have been extracted from the GDEMs and GPS DEM. Nine types of streams have been identified in the ALOS PALSAR DEM, followed by eight types in the SRTM DEM, and six types in the TanDEM-X. The GPS DEM also identified nine types of streams, but with a lower resolution and distorted shapes as shown in Fig. 9. This suggests that the small number of handheld GPS points was not enough to cover the study area. However, with more densification of the GPS points, the resolution of the GPS DEM will give a better horizontal accuracy.

4.4. Criteria for optimizing the GDEM for the study area

Three main criteria were formulated to measure the suitability of the best GDEMs for the study area including the RMSE, the outlier and the number of extracted stream orders from the watershed maps. The best first and third criteria give a full mark of 33.33 out of 100 and the rest is calculated directly or inversely according to the best one. Whereas, the second criterion is divided into three parts and each gives 11.11 out of 33.33, because that all of them are related to outlier detection.

Table 5
Elevation of the GCPs (or BMs) versus obtained heights via GDEMs.

No.	Code	Elevation of GCPs (m)	ALOS PALSAR		SRTM		TanDEM-X	
			H (m)	Discrepancy[a] (m)	h (m)	Discrepancy[b] (m)	H (m)	Discrepancy (m)
1	35−10	872.45	878	6	870	−2	880	0
2	35−12	707.16	714	7	704	−3	715	0
3	35−17	867.16	876	9	865	−2	876	0
4	36−30	513.48	522	9	514	1	522	2
5	36−43	684.65	690	5	681	−4	691	−2
6	43−11	512.95	521	8	511	−2	522	0
7	43−12	640.11	650	**10**[c]	636	−4	649	−2
8	43−17	650.26	661	**11**[c]	646	−4	660	−2
9	36−34	695.96	699	3	689	−7	692	**−11**[c]
10	10016	1232.70	1226	−7	1215	**−18**[c]	1234	−8
11	10037	614.90	614	−1	607	−8	610	**−11**[c]
12	10039	1118.60	1117	−2	1107	**−12**[c]	1112	**−13**[c]
		RMSE (m)	±7.3	−	±7.6	−	±6.5	−

Note:
[a] The descrepancy is the difference between the height values obtained via the ALOSPALSAR and SRTM DEMs minus the H of the GCPs.
[b] The descrepancy is the difference between the height values obtained via the TanDEM-X minus the h of the GCPs as shown in Table 3.
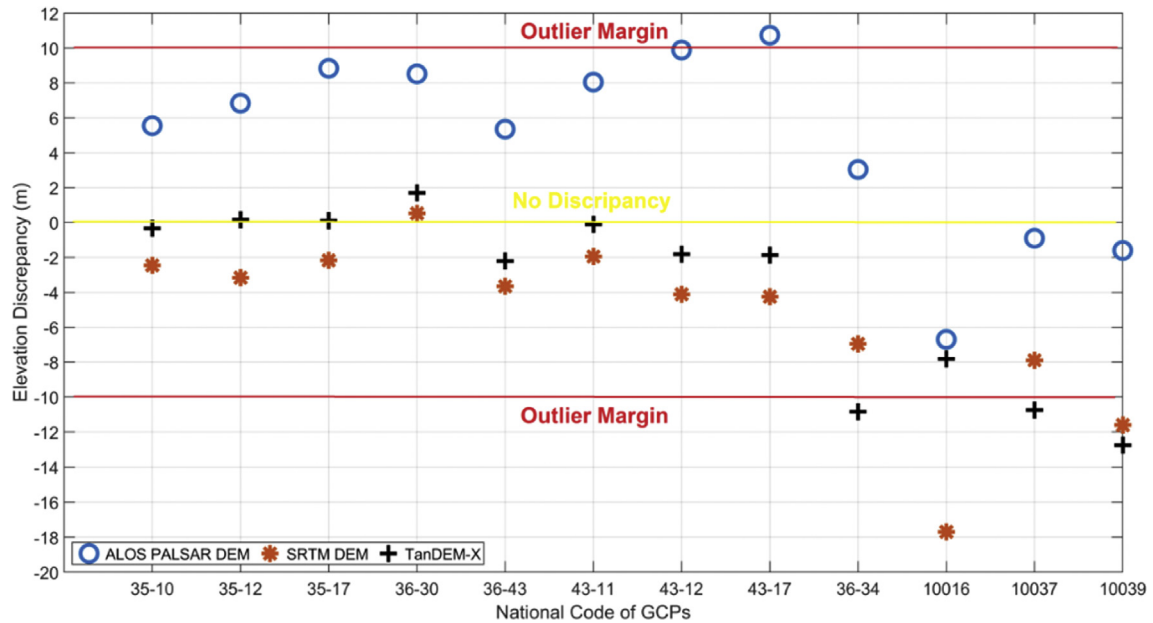[c] The bold values represent the outliers (10 m or greater).

Fig. 8. Absolute elevation discrepancy between the GCPs' elevations and the heights obtained from the GDEMs.

Table 7
Geometric geoid heights of the GCPs in the study area.

No.	Code	h of GCPs (m)	H (m)	N_{Geom}[a] (m)
1	35−10	880.32	872.45	+7.87
2	35−12	714.84	707.16	+7.68
3	35−17	875.9	867.16	+8.74
4	36−30	520.3	513.48	+6.82
5	36−34	702.84	695.96	+6.88
6	36−43	693.2	684.65	+8.55
7	43−11	522.1	512.95	+9.15
8	43−12	650.81	640.11	+10.70
9	43−17	661.86	650.26	+11.60
10	H4	526.63	516.17	+10.46
11	10037	620.8	614.9	+5.86

[a] $N_{Geom} = h - H$.

Meanwhile, both RMSEs (including and excluding the outlier values) of the height values in comparison to the elevation of the GCPs criterion in the TanDEM-X, the outlier percentage of both the

ALOS PALSAR and SRTM DEMs and the number of stream order in the ALOS PALSAR DEM are all given the full point of 33.33. Whereas, the rest DEM points are calculated inversely for RMSEs because the less RMSE value is the best. The same principle is applied to the outlier percentage. In contrast, the full point is given to the largest number of extracted stream order in the ALOS PALSAR DEM and the points of the other DEMs are calculated directly concerning the best one as shown in Table 9.

Accordingly, the best combined horizontal and vertical accuracy of the three GDEMs is followed their resolutions. It can be announced that the ALOS PALSAR DEM 12.5 m is the optimal GDEM for the study area with total points of 90.61 out of 100. However, the total points of both the SRTM DEM 30 m and TanDEM-X 90 m are close together of 78.00 points and 77.35 points, respectively. The total weight ratio precision of three GDEM is 100: 101: 117 respectively (see Table 9). In other words, it can be stated that for each 100 unit obtained accuracy from the TanDEM-X and for the ALOS PALSAR and SRTM DEMs the accuracy increased to 101 and 117 units, respectively.

Table 8
Elevation of the GCPs via the derived DEMs from the GPS points in both cases of adding and without adding N to h.

No.	Code	H_{GCPs} (m)	DEM with adding geoid heights (N)		DEM without adding geoid heights (N)	
			H (m)	Discrepancy (m)	H (m)	Discrepancy (m)
1	35−10	872.45	864	**−8.6**	868	**4.5**
2	35−12	707.16	697	**−10.1**	703	**4.2**
3	35−17	867.16	925	*58.2*	962	*−94.8*
4	36−30	513.48	557	*43.9*	566	*−52.5*
5	36−43	684.65	682	**−2.9**	689	**−4.4**
6	43−11	512.95	509	**−4.2**	518	**−5.0**
7	43−12	640.11	711	*70.5*	671	*−30.9*
8	43−17	650.26	658	**8.2**	657	**−6.7**
9	36−34	695.96	743	*47.2*	733	*−37.0*
10	10016	1232.70	1117	*−115.9*	1068	*164.7*
11	10037	614.90	909	*293.7*	585	*29.9*
12	10039	1118.60	627	*−492.0*	632	*486.6*
	RMSE with outliers (m)	−	−	*179.5*	−	*159.3*
	RMSE without outliers (m)	−	−	8.0	−	5.6

Note: (1) The bold values represent the normal differences between the GCPs and values via the DEM and the italic values are the outliers.
(2) The RMSE of the same points without outliers for the ALOS PALSAR and SRTM DEMs as well as the TanDEM-X are 8.5 m, 3.6 m and 9.2 m respectively.
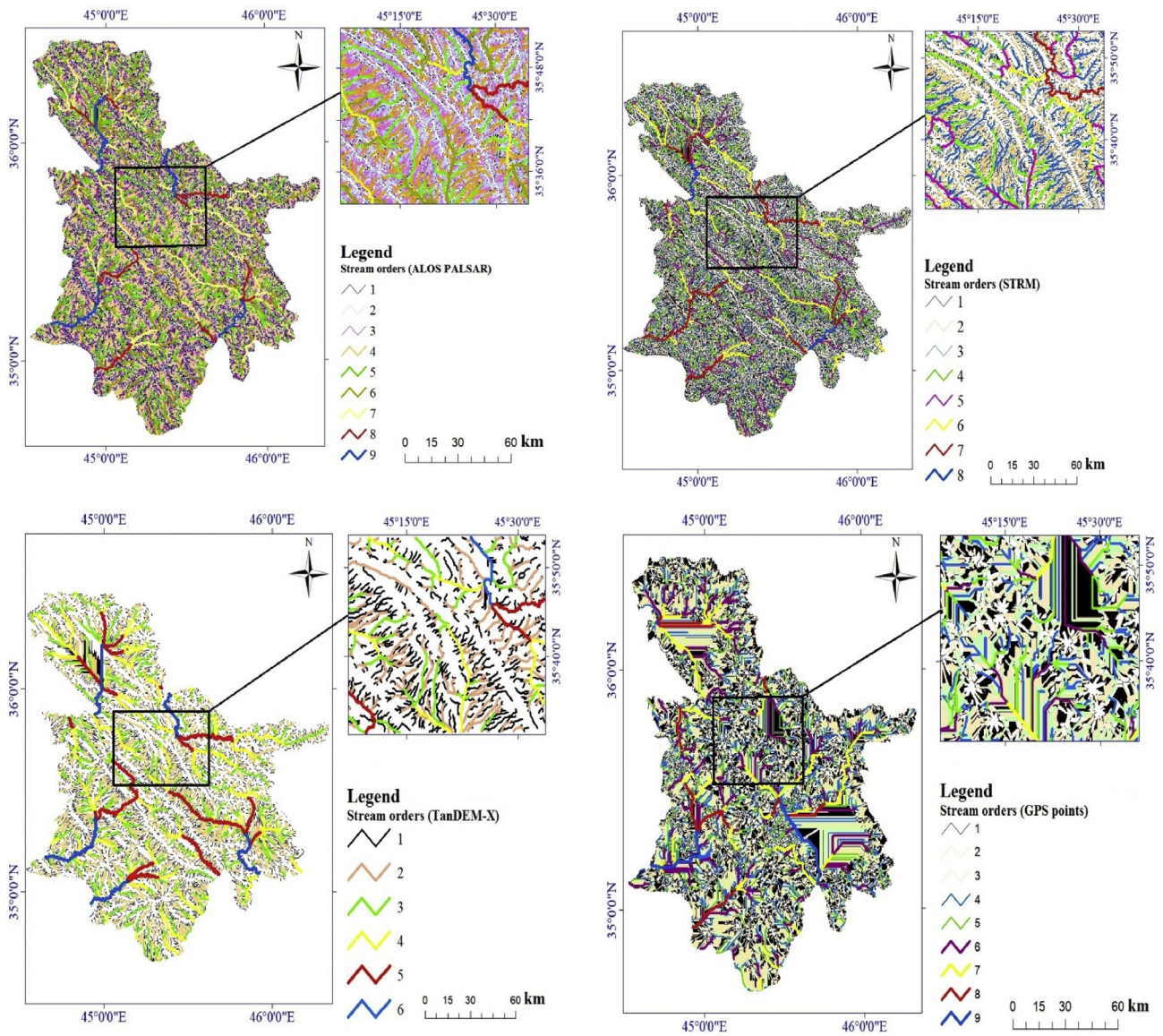
Fig. 9. Extracting the watershed maps from the SRTM and ALOS PALSAR DEMs, TanDEM-X and the derived DEMs from the handheld GPS points for the study area.

Table 9
Formulating the criteria for selecting the optimal GDEM for the study area.

No.	Name of criteria	Criteria values			Criteria points (out of 33.33)		
		ALOS PALSAR (12.5 m)	SRTM (30 m)	TanDEM-X (90 m)	ALOS PALSAR (12.5 m)	SRTM (30 m)	TanDEM-X (90 m)
1	RMSE including outliers (±m)	7.3	7.6	6.5	29.68	28.50	33.33
2	RMSE excluding outliers (±m)	6.4	4.5	3.1	5.38	7.65	11.11
	Outlier percentage (%)	16.7	16.7	25	11.11	11.11	7.42
	Mean deviation of the outliers (m)	0.5	5	1.7	11.11	1.11	3.27
3	No. of the stream order	9	8	6	33.33	29.62	22.22
	Total points (out of 100)	–	–	–	90.61	78.00	77.35
	Combined horizontal and vertical weight	–	–	–	117	101	100

5. Conclusions

Three extracted GDEMs, SRTM DEM, ALOS PALSAR DEM and TanDEM-X, with different resolutions, are validated in the current study based on the three different criteria including the RMSE, outlier detection and the number of extracted stream orders from a watershed map. Indeed, the derived DEMs from the handheld GPS points give better results in comparison to the GDEMs when outliers are discarded.

The horizontal accuracy of the DEMs was tested via watershed maps which are extracted from the each DEM. The results showed that the accuracy of the GDEMs follows their spatial resolutions.

Therefore, more stream types in the watershed map were detected on the ALOS PALSAR DEM than SRTM DEM, which in turn was more accurate than the TanDEM-X. The GPS DEM also detected equal numbers of stream orders as the ALOS PALSAR DEM but with unclear and distorted images, this was due to the limited number of the handheld GPS points that were available to this study.

The vertical accuracy (i.e. heights) of the GDEMs were validated via the GCPs. The RMSE of the height discrepancies of ALOS PALSAR and SRTM DEMs as well as the TanDEM-X show ± 7.3 m, ± 7.6 m and ± 6.5 m, respectively. Results showed that the number of outliers in comparison to the height of 12 GCPs (10 m or more) was 1 (8%) in the TanDEM-X and 2 (16%) in both the ALOS PALSAR and SRTM DEMs.

For validation of the derived DEMs from the GPS points via the GCPs, two DEMs have been derived via EGM2008 for obtaining N values of the points. One DEM was derived through adding N correction to h and another DEM was derived without adding N values. The obtained RMSE of discrepancies with no N correction to the DEM is better than the DEM with N corrected.

Four watershed maps have been extracted from the GDEMs and GPS DEMs. Nine types of streams have been identified in the ALOS PALSAR DEM, followed by eight types in the SRTM DEM, and six types in the TanDEM-X. The GPS DEM also identified nine types of streams.

To sum up, according to the formulated criteria including the RMSE, outlier detection and the number of extracted stream orders from the watershed maps. The best combined horizontal and vertical accuracy of the optimal DEMs for the study area is the ALOS PALSAR DEM 12.5 m. Whereas, the SRTM DEM 30 m and TanDEM-X 90 m ranked the second and third respectively with slight differences between them.

Author statement

Shazad, Tajul, Taher, Ami, Anom and Jwan contributed to the design and formulating the body structure of the research, analyses of the results. Shazad and Taher implemented the handheld GPS survey. All authors participate in writing and revising the manuscript.

Conflicts of interest

The authors declare that there is no conflicts of interest.

References

[1] S. Wise, Effect of differing DEM creation methods on the results from a hydrological model, J. Comp. Geosci. 33 (2007) 1351–1352. Elsevier.
[2] X. Wang, D. Holland, G. Gudmundsson, Accurate coastal DEM generation by merging ASTER GDEM and ICESat/GLAS data over Mertz glacier, Antarctica, J. Rem. Sens. Environ. 206 (2018) 218. Elsevier.
[3] A. Mohammadi, B. Ahmad, H. Shahabi, Extracting digital elevation model (DEM) from sentinel-1 satellite imagery: case study a part of cameron highlands, Pahang, Malaysia, Inter. J. Manag. Appl. Sci. 4 (9) (2018) 109–114. ISSN: 2394-7926.
[4] M. Ouédraogo, A. Degré, C. Debouche, J. Lisein, The evaluation of unmanned aerial system-based photogrammetry and terrestrial laser scanning to generate DEMs of agricultural watersheds, J. Geomorphol. 2014 (2014) 339. Elsevier.
[5] P. Arun, A comparative analysis of different DEM interpolation methods, J. Egypt. J. Rem. Sens. Space Sci. 16 (2013) 133. Elsevier.
[6] S. Mukherjeea, P. Joshi, A. Ghoshb, R. Gargc, A. Mukhopadhyayd, Evaluation of vertical accuracy of open source digital elevation model (DEM), J. Inter. J. Appl. Earth Geoinfo. 21 (2013) 205. Elsevier.
[7] N. D'Ozouville, B. Deffontaines, J. Benveniste, U. Wegmüller, S. Violette, G. De Marsily, DEM generation using ASAR (ENVISAT) for addressing the lack of freshwater ecosystems management, Santa Cruz island, Galapagos, J. Rem. Sens. Environ. 112 (2008) 4131. Elsevier.
[8] L. Drǎguṭab, C. Eisanka, Object representations at multiple scales from digital elevation models, J. Geomorphol. 129 (3–4) (2011) 183–189. Elsevier.
[9] S. Das, P. Patel, S. Singupta, Evaluation of different digital elevation models for analyzing drainge morphometric parameters in mountainous terrain: a case study of the Supin-Upper Tons basin, Sprin. Plus 5 (1) (2016) 1544. Indian Himalayas.
[10] S. Tarquini, S. Vinci, M. Favalli, F. Doumaz, A. Fornaciai, L. Nannipieri, Release of a 10m resolution DEM for the Italian territory: comparison with global-coverage DEMs and an aglyph-mode exploration via the web, J. Comp. Geosci. 38 (2012) 168–170. Elsevier.
[11] C. Rosi, S. Gernhardt, Urban DEM generation, analysis and enhancement using TanDEM-X, J. ISPRS Photogra. Rem. Sens. 85 (2013) 120. Elsevier.
[12] T. Ai, J. Li, A DEM generalization by minor valley branch detection and grid filling, J. ISPRS Photogra. Rem. Sens. 65 (2010) 198. Elsevier.
[13] M. Pa'suya, A. Bakar, A. Din, M. Aziz, M. Samad, M. Mohamad, Accuracy assessment of the Tandem-X DEM in the northwestern of peninsular Malaysia using GPS leveling, ASM Sci. J 12 (2019) 100–106. Special Issue 2 for Malaysia in Space, Section 4.
[14] M. Abdul Halim, G. Pa'suya, R. Narashid, A. Din, Accuracy assessment of TanDEM-X 90m digital elevation model in the east of Malaysia using GNSS/leveling, in: IEEE 10th Control and System Graduate Research Colloquium (ICSGRC 2019) Shah Alam, Malaysia, 2019, pp. 88–93, 2nd – 3rd August.
[15] F. Hebeler, R. Purves, The influence of elevation uncertainty on the derivation of topographic indices, J. Geomorphol. 111 (2009) 4–16. Elsevier.
[16] N. Khalid, A. Din, K. Omar, M. Khanan, A. Omar, A. Hamid, M. Pa'suya, Open-source digital elevation model (DEMs) evaluation with GPS and LiDAR data, Inter. Archiv. Photogram. Rem. Sens. Spat. Inform. Sci. Kuala Lumpur, Malaysia XLII-4/W1 (2016) 299–305.
[17] S. Wise, Assessment the quality for hydrological applications of digital elevation models derived from contours, John Wiley and sons, J. Hydrol. Proc. 14 (2000) 1909–1929.
[18] E. Kaplan, C. Hegarti, Understanding GPS; Principles and Applications, second ed., ARTECH House, Boston, USA, 2006, p. 3.
[19] P. Vaniček, R. Kingdon, M. Santos, Geoid versus quasi geoid: a case of physics versus geometry, J. Contribut. Geophys. Geod. 42 (2012) 102–104.
[20] P. Odera, Y. Fukuda, Y. Kuroishi, A high-resolution gravimetric geoid model for Japan from EGM2008 and local gravity data, J. Earth Planetwo. Space 64 (2012) 361.
[21] W. Torge, Geodesy, third ed., vol. 78, Walter de Gruyter, Berlin, 2001, p. 279.
[22] S. Jalal, R. Bani, Impact of the orientation of residential neighborhoods on optimizing sustainable and equitable exposure of insolation; Case study of Sulaimani, Iraq, Energy Sustain. Develop. 31 (2016) 171. Elsevier.
[23] Ministry of Planning, Regional Planning Board, Existing Development of Sulaymaniyah Governorate in 1990, 1992, p. 17. Study No.975, Baghdad, Iraq (in Arabic).
[24] United Nation (UN), OCHA, Iraq- Sulaymaniyah Governorate Map Action, 2014. Map No. MA012, Iraq.
[25] Government of the Republic of Iraq, The Convention on the Prohibition of the Use, Stockpiling, Production and Transfer of Anti-personnel Mines and on Their Destruction; Request: For an Extension of the Deadline for Completing the Destruction of Anti-personnel Mines in Mined Areas in Accordance with Article 5, Oxford University Press, 2017, p. 25. Version 3.2 August.
[26] A. Setianto, T. Triandini, Comparison of kringing and inverse distance weighted (IDW) interpolation methods in lineament extraction and analysis, J. South. Asian Appl. Geol. 5 (1) (2013) 21–29.
[27] Garmin, Handheld GPS 60cx, 2006.
[28] P. Betoshi, The Detailed Gravity and Magnet Work Study in Sharazoor Area, Kurdistan Region, Iraq, Ph.D. thesis, Department of geology, College of Science, University of Sulaimani, Iraq, 2010, p. 226.
[29] A. Karim, The Gravity and Magnetic Work Surveys at the North East of Chamchamal City- Kurdistan Region, Iraq, Department of geology, College of science, University of Sulaimani, Iraq, 2008, p. 145. M.Sc. thesis.
[30] T. Ameen, A Gravity Survey between Kirkuk and Bazyan and its Geological Implications; Kurdistan Region, Iraq, Department of geology, College of Science, University of Sulaimani, Iraq, 2007, p. 112. M.Sc. thesis.
[31] T. Ameen, Unpublished Terrestrial Gravity Data, 2007.
[32] EGM2008 Website, 2013.
[33] ASTER GDEM validation team, ASTER Global DEM Validation; Summary Report, 2009, p. 3.
[34] A. Jaronski, R. Pozus, The Measurement of Geodetic Control in the Republic of Iraq, Union of Surveying Cartographic and photogrammetric Enterprises, Warszawa, Poland, 1976, pp. 14–15.
[35] Z. Hussein, Accuracy evaluation of digital elevation model created using handheld global positioning system receivers, J. Eng. 22 (6) (2016) 137–148.
[36] G. Zhang, W. Shen, Y. Zhu, Y. Wang, Y. She, Evaluation of ASTER GDEM in the northeastern margin of Tibetan Plateau in gravity reduction, J. Geode. Geodynam. 8 (2017) 335.
[37] R. Wolf, R. Brinker, Elementary Surveying, ninth ed., Harper Collins Publishers, New York, USA, 1994, p. 332.
[38] C. Gupta, V. Gupta, An Introduction to Statistical Methods, 23rd Ed., Vikas Publishing House PVT Ltd., New Delhi, India, 2005, p. 446.

Shazad Jamal Jalal Assistant Professor at College of Engineering, Sulaimani University- Iraq. Date of Birth: April 1972. Education: B.Sc., Surveying Engineering, Department of Surveying, College of Engineering, Baghdad University, Iraq, (1993). M.Sc., Urban and Regional Planning, Center of Urban and Regional Planning for Post Graduate Studies, Baghdad University, Iraq, (2000). PhD student, Geomatics Engineering at University Teknology Malaysia (2018-ongoing). Area of Interest: Geomatics Engineering, Physical Geodesy and Spatial Planning.

Dr. Ami Hassan M Din Senior Lecturer at Faculty of Built Environment and Surveying, University Teknology Malaysia. Date of Birth: February 1983. Education: B.Sc., Geomatics Engineering, University Teknology Malaysia (2007). M.Sc., Geomatics Engineering, University Teknology Malaysia (2010). PhD, Geomatics Engineering, University Teknology Malaysia (2014). Area of Interest: Physcal Geodesy and Hydrography.

Dr. Tajul Ariffin Musa Associate Professor at Faculty of Built Environment and Surveying, University Teknology Malaysia. Date of Birth: September 1972. Education: B.Sc., Land Surveying, University Teknology Malaysia (1995). M.Sc., Land Surveying, University Teknology Malaysia (1997). PhD, Satellite Navigation and Positioning, University of New South Wales, Australia, (2007). Area of Interest: Space Geodesy and Positioning.

Dr. Wan Anom Wan Aris Lecturer at Faculty of Built Environment and Surveying, University Teknology Malaysia. Date of Birth: August 1985. Education: B.Sc., Geomatics Engineering, University Teknology Malaysia (2008). M.Sc., Geomatics Engineering, University Teknology Malaysia (2011). PhD, Geomatics Engineering, University Teknology Malaysia (2018). Area of Interest: Space Geodesy and Geodynamics.

Taher Hama Ameen PhD student, Geophysics, Department of Physics and Astronomy, University of Arkansas at Little Rock (UALR), AR, USA (2016 - ongoing). Assistant Lecturer at College of Science, University of Sulaimani, Iraq (2007—2016). Date of Birth: October 1972. Education: B.Sc., Geology, Department of Geology, College of Science, Salahuddin University, Erbil, Iraq, (1993). M.Sc., Gravity surveys, Geophysics, University of Sulaimani, Iraq, (2007). Area of Interest: Geophysical Investigations, Ground Penetrating radar (GPR) for the Highway and Geotechnical applications.

Jwan Mohammad Ebrahim Designer and Chief surveyor engineer at SALP Middle East Ltd. for pipeline construction. Date of Birth: March 1985. Education: B.Sc., Surveying Engineering, Department of Surveying, College of Engineering, Aleppo University, Syria, (2007). Area of Interest: GPS observation and UAV mapping, design of roads and pipelines.